High-Resolution Infrared Spectroscopic Measurements of Comet 2P/Encke: Unusual Organic Composition and Low Rotational Temperatures

Yana L. Radeva[1,2], Michael J. Mumma[2], Geronimo L. Villanueva[1,2], Boncho P. Bonev[1,2], Michael A. DiSanti[2], Michael F. A'Hearn[3], Neil Dello Russo[4]

---

[1]Department of Physics, Catholic University of America, Washington, DC 20064;

yanaradeva@gmail.com

[2]Goddard Center for Astrobiology, NASA Goddard Space Flight Center, Greenbelt, MD 20771

[3]Department of Astronomy, University of Maryland, College Park, MD 20742

[4]The Johns Hopkins University Applied Physics Laboratory, Laurel, MD 20723

Number of manuscript pages: 42

Number of figures: 6

Number of tables: 3

Running head: The Organic Composition of Comet 2P/Encke

Corresponding author: Yana L. Radeva

NASA Goddard Space Flight Center, Mailstop 690.3

Greenbelt, MD 20771

yanaradeva@gmail.com

Key words: COMETS, COMPOSITION; COMET 2P/ENCKE; INFRARED OBSERVATIONS; ORIGIN, SOLAR SYSTEM; SPECTROSCOPY

Abstract

We present high-resolution infrared spectroscopic measurements of the ecliptic comet 2P/Encke, observed on 4-6 Nov. 2003 during its close approach to the Earth, using the Near Infrared Echelle Spectrograph on the Keck II telescope. We present flux-calibrated spectra, production rates, and mixing ratios for H_2O, CH_3OH, HCN, H_2CO, C_2H_2, C_2H_6, CH_4 and CO. Comet 2P/Encke is a dynamical end-member among comets because of its short period of 3.3 years. Relative to "organics-normal" comets, we determined that 2P/Encke is depleted in HCN, H_2CO, C_2H_2, C_2H_6, CH_4 and CO, but it is enriched in CH_3OH. We compared mixing ratios of these organic species measured on separate dates, and we see no evidence of macroscopic chemical heterogeneity in the nucleus of 2P/Encke, however, this conclusion is limited by sparse temporal sampling. The depleted abundances of most measured species suggest that 2P/Encke may have formed closer to the young Sun, before its insertion to the Kuiper belt, compared with "organics-normal" comets – as was previously suggested for other depleted comets (e.g. C/1999 S4 (LINEAR)). We measured very low rotational temperatures of 20 - 30 K for H_2O, CH_3OH and HCN in the near nucleus region of 2P/Encke, which correlate with one of the lowest cometary gas production rates (~ 2.6×10^{27} molecules s^{-1}) measured thus far in the infrared. This suggests that we are seeing the effects of more efficient radiative cooling, insufficient collisional excitation, and/or inefficient heating by fast H-atoms (and icy grains) in the observed region of the coma. Its extremely short orbital period, very low gas production rate, and classification as an ecliptic comet, make 2P/Encke an important addition to our growing database, and contribute significantly to the establishment of a chemical taxonomy of comets.

1. INTRODUCTION

The establishment of a taxonomic classification for comets based on their chemical composition is essential to understanding the formation and evolution of our Solar System (for a recent review, see Mumma & Charnley 2011). Comets are relatively unaltered remnants from the creation of the Solar System 4.6 billion years ago, and are currently found in two major dynamical reservoirs: the Kuiper belt and the Oort cloud (Gladman 2005).

The dynamical classification of a comet is based on its orbital Tisserand invariant with respect to Jupiter (T_j). For Jupiter-family comets: $2 < T_j < 3$; for Chiron-type comets: $T_j > 3$ & $a > a_j$; for Encke-type comets: $T_j > 3$ & $a < a_j$; and for nearly isotropic (i.e., Oort cloud) comets: $-2 < T_j < 2$, where "a" is the semi-major axis of a comet (Levison 1996). Identifying the long-term dynamical reservoir of a comet does not, however, identify its formative region. The "*Nice*" model predicts significant dynamical dispersion of icy bodies in the outer proto-planetary disk (Tsiganis et al. 2005), and while it suggests that comets currently found in the Kuiper belt formed beyond 5 AU from the Sun, the newer "Grand Tack" model (Walsh et al. 2011) points to the possible origin of many Kuiper belt and Oort cloud comets in the terrestrial planets region. Another new model (Levison 2010) questions whether all Oort cloud comets indeed formed in our proto-planetary disk, and suggests that many may have been captured after ejection from the proto-planetary disks of other stars in the Sun's birth cluster. Clearly, a different metric is needed to clarify a comet's formative region.

Current models for the protoplanetary disk suggest the presence of strong radial gradients in chemistry and temperature, and direct sampling of cometary material confirms the presence of pre-cometary grains that formed over extremely diverse conditions, ranging from the interstellar

medium to the near-Sun inner planetary region (Brownlee et al. 2006). These models also predict compositional and isotopic diversity amongst the ices formed in different regions, and thus in comet nuclei that accumulated from them. The recent discovery of ocean-like water in the ecliptic comet 103P/Hartley 2 (Hartogh et al. 2011) emphasizes this diversity, re-opens the question of the role of comets in delivering Earth's water, and makes the need for a robust compositional taxonomy even more compelling.

Optical surveys of product species (such as OH, CN, NH, C_2, C_3, etc.) revealed that the fraction of comets depleted in C_2 and C_3 radicals (relative to CN) is greater among Jupiter family comets than among Oort cloud comets (A'Hearn et al. 1995, Fink 2009, Langland-Shula & Smith 2011, Cochran et al. 2012). However, it is often problematic to uniquely interpret the origin of product species. They can originate from the photo-dissociation of primary (a.k.a. parent) volatiles (i.e., species native to the cometary nucleus and released under the influence of solar radiation), from refractory grains, or even from chemical processes in the coma. Thus, there are multiple possible (and unknown) pathways and parents for each observed radical. Also, comets that are termed 'typical' in product species (C_2, C_3, CN) are sometimes not "organics-normal" in their primary volatile composition (8P/Tuttle, Bonev et al. 2008; 10P/Tempel 2, Paganini et al. 2012; 9P/Tempel 1, Mumma et al. 2005; 6P/d'Arrest, Dello Russo et al. 2009). In short, it is critically important to develop a chemical taxonomy based on primary volatile composition.

Infrared and radio spectroscopic observations of comets enable the measurement of gas production rates of primary volatile species. These surveys now permit quantitative sampling of eight or more primary species at infrared wavelengths, simultaneously with water, the (usually) dominant species. Several important primary volatiles (e.g., CH_4, C_2H_2, C_2H_6, etc.) are readily measured at infrared wavelengths, but (being symmetric) their pure rotational transitions are

forbidden and so they cannot be observed at mm and sub-mm wavelengths. Radio observations are, however, very useful in studying the rotational transitions of more complex molecules (provided that they have a permanent dipole moment), and are thus complementary to infrared studies.

Our group has identified "organics-enriched", "organics-normal", and "organics-depleted" comets on the basis of mixing ratios of organic volatiles, such as CH_3OH, HCN, H_2CO, C_2H_2, C_2H_6, CH_4, and CO (Mumma et al. 2003; Crovisier et al. 2007; DiSanti and Mumma 2008). The Oort cloud comets C/2001 A2 (LINEAR) (Magee-Sauer et al. 2008), and C/2007 W1 (Boattini) (Villanueva et al. 2011a) have been identified as enriched in most organic species, and the Oort cloud comet C/1999 S4 (LINEAR) (Mumma et al. 2001; 2003) has been identified as severely depleted in most organics. Among ecliptic comets, 17P/Holmes is enriched (Salyk et al. 2007, Dello Russo et al. 2008) and 73P/Schwassman-Wachmann-3 is severely depleted (Villanueva et al. 2006, Dello Russo et al. 2007). However, 17P/Holmes was observed while outbursting at ~2.4 AU (most comets are observed much closer to the Sun). It is likely that a fraction of the water in its inner coma was ejected in the form of ice (Yang et al. 2009), which (if depleted in organics) could cause enrichment in the organic gases measured at infrared wavelengths. Such polar and apolar ices were identified recently in comets 103P/Hartley 2, C/2006 W1 (Boattini), and 10P/Tempel 2 (Mumma et al. 2011, Villanueva et al. 2011a, Paganini et al. 2012). Chemical diversity is found in each dynamical reservoir, and a more expansive sample of comets from both the Kuiper belt and the Oort cloud is needed in order to identify the true origin of an individual comet and the fractional representation of taxonomic classes within each dynamical reservoir.

Here we present the organic composition of the ecliptic comet 2P/Encke, and discuss its organic depletion, its low rotational temperatures, and aspects of its possible origins. 2P/Encke (hereafter

Encke) is the prototypical "Encke-type" comet, with T_J = 3.025, period of 3.3 years, and aphelion distance of 4.09 AU. Encke's aphelion distance is unusually small, and dynamical simulations suggest that the comet may have been in a dormant state for a long period of time, after it became dynamically decoupled from Jupiter (Levison et al. 2006). Encke was discovered in 1786 by Méchain, at the Paris Observatory, and up to the time of our observations, it had returned to perihelion 67 times since its discovery (Sekanina 1991).

2. OBSERVATIONS AND DATA REDUCTION

Comet Encke reached closest approach to Earth (with Δ = 0.261 AU) on 17 Nov. 2003, and perihelion (q = 0.338 AU) on 30 Dec. 2003. We characterized the comet on 4-6 Nov. 2003 (Table 1), using the cross-dispersed Near Infrared Echelle Spectrograph (NIRSPEC) at Keck-II atop Mauna Kea, HI. NIRSPEC has a 1024 x 1024 InSb detector array; and provides resolving power $\lambda/\Delta\lambda \sim 25000$ when using the 0.432″ entrance slit. A single spectral frame (covering 1024 x 1024 pixels) samples multiple echelle orders, e.g., orders 21-26 in the KL2 grating setting; and orders 22-27 in the KL1 grating setting (Table 1). This large spectral grasp is one of the main strengths of NIRSPEC since the simultaneous detection of multiple organic species and water minimizes numerous systematic uncertainties. The slit has a length of 24", corresponding to 121 pixels of 0.198" each in the spatial direction.

We nodded the telescope by 12" (± 6" along the instrument slit) in a sequence A1, B1, B2, A2 (where A and B correspond to the two different positions of the comet in the slit). The difference in frames (A1–B1–B2+A2) and the further combination of the A and B beams cancels dark current and telescope thermal background, as well as sky emission lines (to second order in a Taylor series expansion about the mean air mass). We cropped individual echelle orders from the difference frame and (after flat field division) "masked" them in order to remove hot pixels and

cosmic ray hits. We re-sampled the data in the spatial and spectral directions, correcting for the initial tilt, to ensure that (in the re-sampled data) the pixels along each column correspond to a common frequency and that all pixels along a given row sample a common spatial position in the coma.

We generated terrestrial transmittance spectra using our adapted (Villanueva et al. 2011b) version of the LBLRTM (Layer-by-Layer Radiative Transfer Model, Clough et al. 2005) spectral synthesis program, and convolved the fully resolved synthetic spectra to the instrumental resolution in order to determine the telluric abundances of H_2O, CO_2, O_3, N_2O, CO, C_2H_6 and CH_4 (by matching the synthetic and measured spectrum, through an iterative fitting process). We performed frequency calibration of the data by aligning modeled sky emission lines with those observed in the data frames. We scaled the convolved (to $\lambda/\Delta\lambda \sim 25000$) telluric model to the cometary continuum level; subtracting this isolated the residual emission spectrum of the comet, still multiplied by the atmospheric transmittance function. The fully-resolved best-fit model provided a precise value for the transmittance at each Doppler-shifted line position. We used spectra of a flux standard star to convert the counts per second in the comet data to flux density in W m^{-2} $[cm^{-1}]^{-1}$. Detailed descriptions of our standard data analysis procedures are given in the literature (e.g., Radeva 2010, Villanueva et al. 2009, Bonev 2005, DiSanti et al. 2001, and references therein).

3. RESULTS

We present quantitative results for H_2O, CH_3OH, HCN, H_2CO, C_2H_2, C_2H_6, CH_4, and CO (Table 2) in comet Encke. We present production rates for five species (H_2O, CH_3OH, HCN, C_2H_6, and CH_4), 3-σ upper limits for three others (CO, H_2CO, C_2H_2), and rotational temperatures for H_2O,

CH_3OH and HCN. We give mixing ratios for all trace species (production rates of organic species as percentages relative to water), for the three dates of observation. Results for Encke are compared with those for other comets in Table 3.

3.1. Spectral Gallery

Figure 1 presents a nucleus-centered, flux-calibrated spectral extract, which contains the spatially summed signal from nine spatial pixels centered on the nucleus, spanning a range of 1.78″ (~ 387 km). The synthetic model of the terrestrial atmosphere is shown as a dashed line (superimposed on the cometary spectrum) in the upper panel of the figure. The corresponding residual spectrum of H_2O (after subtraction of the transmittance model from the measured cometary spectrum) is shown in the lower panel, with the ± 1-σ noise envelope superimposed (dashed line). The noise envelope is largest at frequencies that correspond to sky emission lines (compare the upper and lower panels of Fig. 1). Figures 1-18 in the Electronic Supplementary Material present all remaining spectral orders for the three dates of observation.

3.2. Measured Rotational Temperatures

At infrared wavelengths, we sample the innermost coma over a range in nucleus-centered distance that depends on the comet's geocentric distance (see Table 1). In this inner region, collisions thermalize the rotational populations (P_m) of the ground vibrational level of each molecule (Xie and Mumma 1992), and a rotational temperature (T_{rot}) is extracted to model these populations: $P_m = \frac{g_m \exp(-E_m / kT_{rot})}{Z(T_{rot})}$, where g_m is the statistical weight of level 'm', E_m is the energy of the level, and Z is the partition function. For Encke at the time of observation, the 1.78" nucleus-centered extract spanned 387 km at the comet, corresponding to ± 194 km from the nucleus, as projected onto the sky plane. The number density of molecules at ~ 194 km from

the nucleus was approximately 8 x 10^6 cm^{-3} (for Q_{gas} ~ 3 x 10^{27} s^{-1}, see Discussion, §4). For a more active comet, the same number density would be measured at a greater distance from the nucleus, e.g., at ~ 346 km, even for the modestly productive comet C/2007 W1 (Boattini) (Q ~ 1.2 x 10^{28} s^{-1}). Under these conditions, the rotational population of H_2O in C/2007 W1 (Boattini) was well thermalized (retrieved T_{rot} ~ 80 K) (Villanueva et al. 2011a), and in comet Encke the rotational population should be thermalized for all higher densities (i.e., within the sampled 1.78" nucleus-centered extract).

Accurate rotational temperatures are vital for calculating production rates of detected species, especially given that most measurements sample only a sub-set of ro-vibrational levels. To extract a rotational temperature for a given molecule, we compare the ratios of measured intensity and modeled fluorescence efficiency factor (g-factor) for the sampled spectral lines. The g-factors (in photons $molecule^{-1}$ s^{-1}) predict the intensity of each line at a given T_{rot}. Therefore, the temperature that most accurately describes the rotational level populations should provide the best agreement, within error, for the ratios of flux/g-factor for the measured lines. For the present analyses, we used the improved solar model and improved fluorescence models developed by our group (see Villanueva et al. 2011a (Boattini - solar & fluorescence models); 2012a (H_2O); 2012b (CH_3OH), and original sources cited therein).

The excitation analyses for three molecular species are shown in Fig. 2. They demonstrate our approach and the agreement (within error) among production rates obtained from individual lines at the retrieved (optimized) T_{rot}, that corresponds to the solution with zero slope. The rotational temperatures derived for water, methanol, and hydrogen cyanide in Encke agree within experimental error (Table 2): T_{rot} (H_2O) = $29^{-7}/_{+10}$ K (4 Nov., KL1 setting), T_{rot} (H_2O) = $30^{-2}/_{+2}$ K (5 Nov., KL1 setting), T_{rot} (CH_3OH) = $24^{-5}/_{+6}$ K (5 Nov., KL1 setting), and T_{rot} (HCN) = 20 -

$^{8}/_{+16}$ K (6 Nov., KL2 setting). These temperatures are much lower than those we normally obtain for the inner coma of comets (see Discussion, §4). Fig. 3 illustrates the fit of the synthetic fluorescence models (convolved with modeled terrestrial transmittance) to the cometary spectra at each T_{rot}. The rotational temperatures retrieved from H_2O on the respective dates of observation were adopted for other species, for which T_{rot} could not be extracted due to an insufficient spread of excitation energies amongst the measured lines.

Our approach assumes that the observed medium is optically thin at infrared wavelengths. Optical depth effects must be considered for very active comets such as Ikeya-Zhang or Hale-Bopp (Dello Russo et al. 2004, DiSanti et al. 2001). In Encke, optical depth effects are negligible because the comet has very low gas production rates – $Q(H_2O)$ is about 100 times smaller in Encke than in Ikeya-Zhang, and about 1000 times less than in Hale-Bopp.

3.3 Production Rates

We extracted a production rate Q_i from each measured spectral line, assuming spherical outflow with uniform velocity. Then, $Q_i = \frac{4\pi\Delta^2 F_i}{g_i \tau (hc\upsilon) t_i f(x)}$, where F_i is the flux of the i^{th} line collected from a box on the sky centered on the nucleus and measuring 0.432" (slit-width) x 1.782" (extract length). Other parameters include the geocentric distance Δ [meters], the terrestrial transmittance (t_i) at the frequency of the i^{th} line; the fraction (f(x)) of the total coma content of the targeted species sampled by the beam; the energy ($hc\nu$) of a photon with wavenumber ν (cm^{-1}) the line g-factor (g_i) at T_{rot}; the molecular lifetime (τ); and the assumed expansion velocity (0.8 x $R_h^{-0.5}$ km s^{-1}) (cf., Mumma et al. 2003). The weighted-mean production rate for each species is calculated from the individual production rates obtained from the sampled lines (using the

retrieved rotational temperature), where the weight is the inverse of the respective squared stochastic error for a given line (cf. Fig. 2).

We first derive production rates from nucleus-centered extracts (which provide the highest signal-to-noise ratio), but the 'nucleus-centered' Q underestimates the 'global', or 'terminal', production rate owing to loss of flux in the instrumental slit (as a result of seeing effects or comet drift in the slit, etc.). Therefore, we determine the mean values of production rates (symmetric Qs) from extracts equidistant on both sides of the measured spatial intensity profile (Figure 4) – these reach a terminal value at ~ 1″ from the nucleus. We calculate a growth factor for each species, as the ratio between the terminal and nucleus-centered production rate. Some molecules do not have sufficient signal-to-noise ratio away from the nucleus, which requires adopting a growth factor (usually from H_2O, measured simultaneously, in the same setting), for the calculation of their terminal production rates. This procedure (averaging of production rates) also corrects for 1-dimensional asymmetries in the gas outflow (Xie and Mumma 1996a, 1996b).

We retrieved production rates for H_2O in the KL1, KL2, and MW_A setting, and for the following organic species: CH_3OH, HCN, H_2CO, C_2H_2, C_2H_6 (ν_5 and ν_7 bands), CH_4 and CO. We present 3-σ upper limits for those species for which we cannot claim a firm detection: H_2CO on 4 & 6 Nov.; C_2H_2 on 4 & 6 Nov.; C_2H_6 (ν_5 band) on 6 Nov., and CO on 5 & 6 Nov. CO measurements were combined from 5 & 6 Nov. to improve the signal-to-noise ratio, given the limited time on source in the MW_A setting. The instrumental setting, time on source, global production rate and mixing ratio for each molecule is presented in Table 2. The production rates of the dominant volatile - water, agree within 2-σ on all three dates, and for all three settings used.

4. DISCUSSION

Our high-resolution infrared spectra of comet Encke on three consecutive dates reveal its unusual composition, and very low rotational temperatures consistent with its low water production rate. 6P/d'Arrest is another example of a comet with a very low production rate (comparable to that of Encke), which is also characterized by low rotational temperatures (30-50 K) (Dello Russo et al. 2009). The local collisional excitation rate (c) is directly proportional to the production rate of a comet, according to: $c = n\sigma v_t$, where n is the number density ($n \sim \frac{Q}{4\pi v_o r^2}$), σ is the collisional cross-section for excitation, v_t is the thermal velocity, and v_o is the gas outflow velocity (Weaver and Mumma 1984). Is it possible that the low rotational temperatures observed in comet Encke are the signature of relaxation by radiative decay dominating collisions in controlling its rotational level population?

Xie and Mumma (1992) examined this question in a detailed study of water in comet 1P/Halley that included collisions of electrons with water, water with water, infrared fluorescent pumping of H_2O with rotational cascade, and radiative decay of H_2O rotational levels. They applied their model for conditions measured during the *Giotto* coma flythrough (14 March 1986; 0.9 AU). For a water production rate of 5 x 10^{29} s^{-1} and kinetic temperature of 60 K, they evaluated the excitation & de-excitation rates over the nucleocentric distance range of 1000 km to 3 x 10^5 km. In their model, the water density was ~ 6 x 10^6 cm^{-3} at 3000 km, well within the coma region where H_2O rotational emission lines are optically-thick and radiative trapping reduces the escape-to-space probability significantly. Xie and Mumma (1992) showed that electron and neutral-neutral collisions dominate rotational excitation and de-excitation of water under such conditions. Since cross-sections and radiative decay times are similar for other polar gases

(CH_3OH, H_2CO, HCN, CO), we expect they too will be controlled by collisions. Radiative decay rates are zero for apolar gases (CH_4, C_2H_6, etc.), so collisions will control their rotational temperatures so long as fluorescent pumping rates remain small. This is true within the volume sampled in our investigation, since the pumping rates for all molecules are less than one event per 1000 seconds. For conditions in 2P/Encke ($Q = 2.6 \times 10^{27}$ s^{-1}, $v_0 \sim 0.8$ km/s), the density of 6×10^6 cm^{-3} is reached at ~200 km nucleocentric distance. Most of the molecules sampled in our beam fall within this distance range. We therefore conclude that rotational populations in all molecules sampled in this study (Table 2) are controlled by collisions.

In an attempt to explain the high rotational temperatures found in the near nucleus region of 73P/Schwassmann-Wachmann 3, Fougere et al. 2012 suggest that sublimation of water from warm grains introduced excess heat to the near-nucleus coma, thus preventing adiabatic cooling of the expanding gas and maintaining rotational temperatures far above the adiabatic limit. A similar effect is consistent with the release of water-rich icy grains in C/2006 W1 (Boattini), as inferred from the distinct spatial distributions of polar and apolar volatiles in the coma (Villanueva et al. 2011a). Moreover, our observed (unusual) depletions of primary volatiles in Encke, and its unusual thermal history, suggest that release of ice-mantled grains (and the concomitant excess heat injected by sublimation) is not likely. Thus, we may be seeing the expected adiabatic cooling of expanding gas.

We must also consider the effects of low thermalization efficiency of fast H-atoms, which are by-products of H_2O and OH photodissociation, and whose thermalization increases the temperature of the coma (for comets with high gas production rates) after the initial temperature decrease introduced by expansive adiabatic cooling (Combi et al. 2004). However, re-heating

normally operates at greater nucleocentric distances than we sampled in Encke. A detailed evaluation of these competing effects is deferred to a future publication.

Historically, Encke's spectral continuum at optical wavelengths has long been noted as unusual. Optical observations demonstrate a very weak continuum consistent with a deficiency of sub-micrometer sized dust in Encke. This behavior and observations of a strong thermal IR continuum (Ney 1974, Campins et al. 1982) were argued to imply a lower than typical fraction of small dust particles in Encke's coma (i.e., most dust particles had radii between 5 and 10 μm, or even > 20 μm) (Gehrz & Ney 1989, Jewitt et al. 2004, Lisse et al. 2004). We observed a strong infrared continuum, consistent with a substantial contribution from micron-sized grains.

The gaseous activity of Encke reported here agrees with contemporaneous measurements obtained from the Odin space observatory. Our water production rate in Encke of $(2.6 \pm 0.1) \times 10^{27}$ s^{-1} (weighted mean from all settings, 4-6 Nov.) at a mean heliocentric distance of 1.2 AU, is, as expected, lower than that measured closer to the Sun: $Q(H_2O) = (4.9 \pm 0.7) \times 10^{27}$ s^{-1}, at R_h of 1.01 AU (16 Nov. 2003), from Odin observations of the 557 GHz line of H_2O (Biver et al. 2007) (although there is agreement at the 3-σ level). Scaling our production rate, to account for differences in heliocentric distance, by R_h^2 (R_h = 1.2 AU), provides agreement at the 1-σ level with Odin measurements.

Encke is an important addition to the growing database of ecliptic comets that have been characterized at infrared wavelengths. Its composition is unusual in being depleted in most organic species (HCN, H_2CO, C_2H_2, C_2H_6, CH_4, and CO) but enriched in CH_3OH. The weighted-mean mixing ratios for measured species are presented in Table 3, along with those of other Jupiter-family comets (21P/Giacobini-Zinner, 73P/Schwassman-Wachmann-3, 9P/Tempel 1,

6P/d'Arrest, 10P/Tempel 2 and 17P/Holmes) and three Oort cloud (current) 'end-member' comets (the severely depleted C/1999 S4 (LINEAR), and the significantly enriched comets C/2001 A2 (LINEAR) and C/2007 W1 (Boattini)). The only organics-enriched member of the presented Jupiter-family group is 17P/Holmes, whose enrichment is most likely overestimated, given its heliocentric distance of observation (2.4 AU) – where water in the inner coma is more likely in the form of ice (as previously discussed (§1)). Table 3 indicates that: (1) the number of ecliptic comets observed at infrared wavelengths is insufficient for statistical analysis, and no clear trends are seen in the current sample; (2) Encke is the ecliptic comet with highest methanol mixing ratio, studied in the infrared.

Encke's composition is also presented in Fig. 5, in comparison to that of the severely depleted JFC 73P/Schwassman-Wachmann-3C (hereafter 73P/S-W 3-C), the severely depleted C/1999 S4 (LINEAR) (hereafter C/1999 S4), and the enriched C/2001 A2 (LINEAR) (hereafter C/2001 A2) and C/2007 W1 (Boattini). Fig. 5 clearly illustrates the significant depletion of Encke in HCN, H_2CO, C_2H_2 & CO; its moderate depletion in C_2H_6 and CH_4; and its enrichment in CH_3OH.

Our weighted mean mixing ratios (from different dates) for CH_3OH (3.48 $\pm$ 0.27%), H_2CO (< 0.13% at 3-σ), and HCN (0.09 $\pm$ 0.01%) in Encke are consistent with those measured at radio wavelengths: CH_3OH (4.1%), H_2CO (< 1.4 %, 3-σ), and HCN (0.09%) (Crovisier et al. 2007). Infrared and radio measurements both indicate enrichment of Encke in CH_3OH and depletion in HCN, and our infrared measurements alone indicate depletion in CH_4, C_2H_2, C_2H_6, H_2CO and CO. By contrast, optical observations of a sample of 85 comets found Encke to be 'typical' in carbon-chain molecules (A'Hearn et al. 1995; see also Fink et al. 2009), but Cochran et al. (2012) find Encke to be CH/CN-enriched. However, the product species sampled at optical wavelengths can have multiple origins (including release from grains), which greatly complicates

drawing cosmogonic implications from their measured abundance ratios. One possible explanation for the discrepancy between infrared (confirmed by radio) and optical measurements is that some carbon-chain parent molecules not sampled in the infrared may be more abundant in Encke, resulting in typical values for C_2 and C_3 but depletion in C_2H_6 and C_2H_2 (acetylene is a possible parent of C_2, but C_2H_6 is not (Weiler 2012)). Several other comets also show discordant comparisons in product and primary volatile (i.e., potential parent) species (§1).

It is very difficult to determine whether the depletion of 2P/Encke is evolutionary or primordial. Successive depletion during its numerous orbits around the Sun could have induced preferential loss of the most volatile ices (CO and CH_4, having sublimation temperatures of 25 K and 31 K, respectively) over those having higher sublimation temperatures (e.g., CH_3OH, 99 K) (Yamamoto 1985). For example, ecliptic comet 73P/S-W 3-C, has a short period (5.4 years) and is a severely depleted end-member. However, the ecliptic comet 103P/Hartley 2 (P = 6.5 years) is normal in its organic primary composition (although depleted in C_2H_2, and highly enriched in CO_2 (A'Hearn et al. 2011)), and 'typical' in its product species. Taken together, these 3 examples suggest that something other than evolutionary processing (e.g., formative conditions) influenced current volatile compositions, although Encke with its very short orbital period and small perihelion distance may represent a special case.

It is possible that if an ecliptic comet formed later in the Solar System's evolutionary timeline than did Encke, more ionizing x-ray flux from the Sun would reach greater distances thanks to nebular clearing, and the resulting higher H-atom densities – combined with lower temperatures enhancing H-retention on the surfaces of grains – would increase the efficiency of H-atom addition reactions (e.g., more C_2H_6 would form from C_2H_2, and CH_3OH from CO; see below). The conversion efficiency for C_2H_2 into C_2H_6 can be calculated as $C_2H_6/(C_2H_2 + C_2H_6)$, and is >

0.8 in Encke. This relatively high value could result from formation in a region with higher H-atom densities, and/or lower temperatures, than were experienced by comets with a lower C_2H_2 hydrogenation efficiency. High hydrogenation efficiency is also consistent with the low upper limits for CO & H_2CO, but significant enrichment of CH_3OH in Encke: $(H_2CO + CH_3OH)/(CO + H_2CO + CH_3OH) > 0.7$. Alternatively, a high initial endowment of CO with low conversion to H_2CO and CH_3OH could indicate that the 'missing' CO (the most volatile species) was lost during Encke's numerous orbits around the Sun. The relatively efficient conversion implied for C_2H_2 (to ethane) may also suggest that most CO that condensed onto its pre-cometary grains later converted to CH_3OH. If true, the severe depletion of CH_3OH in C/1999 S4 together with its enrichment in Encke is consistent with this view.

It is important to note that comet Encke is not as severely depleted as C/1999 S4, which comes from the Oort cloud and is considered to be dynamically new. It was previously suggested that C/1999 S4 is depleted because it likely formed closer to the young Sun than 'organics-normal' comets (Mumma et al. 2001). That is a possible explanation for comet Encke's depletion as well, but if so it probably formed farther from the Sun than did C/1999 S4, given Encke's less severe depletion.

In addition to heliocentric distance, other factors must be considered to explain the depletion (or enrichment) of a cometary nucleus, such as localized heating, or formation of the nucleus from fractions originating in regions with diverse chemical composition. Our quantitative production rates on three consecutive dates can test for potential heterogeneity of Encke's nucleus. If the nucleus were heterogeneous, we would expect to see variability in the measured mixing ratios as it rotates and different vents are sequentially activated under the influence of solar radiation (depending on the size of the fractions, locations of vents, etc.). The rotation period of Encke was

measured to be 11.056 ± 0.024 h (sidereal, Jockers et al. 2011), 11.083 ± 0.003 h (synodic, Lowry and Weissman 2007), and 11.079 ± 0.009 h (synodic, Fernández et al. 2005). Our KL2 observations were separated by ~ 47 h 30 m (4.3 rotation periods) and we likely observed release from different regions of Encke's nucleus, but our KL1 observations were separated by ~ 22 h (2.0 periods), and may sample the same region. We present a comparison of the mixing ratios in comet Encke on different dates in Figure 6, and see agreement in the abundances measured for each species within 1-σ (2-σ for HCN). This lack of temporal variability in the measured organic abundances is consistent with compositional homogeneity in the mean volatile release (averaged over all active vents, regardless of possible chemical diversity), similar to comet 103P/Hartley-2 (Mumma et al. 2011, Dello Russo et al. 2011), C/2000 WM_1 (Radeva et al. 2010), and C/2004 Q2 (Bonev et al. 2009). However, our sparse temporal sampling and limited spatial information prevent us from drawing a definitive conclusion on this question.

5. SUMMARY

The ecliptic comet Encke is an important addition to our growing database of comets studied at infrared wavelengths, first, because fewer ecliptic comets have been studied in comparison to Oort cloud comets, and second, because it is a dynamical end-member owing to its very short orbital period of 3.3 years. Our investigation of Encke resulted in the following conclusions:

1. Encke exhibits one of the lowest gas production rates for water among comets in our sample, with $Q(H_2O)$ being $(2.6 \pm 0.1) \times 10^{27}$ s^{-1} (weighted mean from all settings, 4-6 Nov.) at a mean heliocentric distance of 1.2 AU. The scatter among individual measurements is somewhat larger than the error in the mean (Table 2).

2. Encke exhibits very low rotational temperatures in the near-nucleus coma ($T_{rot} \sim 20 - 30$ K, for H_2O, CH_3OH and HCN). Collisions are sufficient to maintain the rotational level populations. The absence of excess heating by water released from icy-mantled grains likely permits the predicted adiabatic cooling of outflowing gas in the near nucleus coma to control the rotational temperature.

3. Encke is depleted in HCN, H_2CO, C_2H_2, C_2H_6, CH_4 and CO, but is enriched in CH_3OH (it being the least volatile primary species other than H_2O). Our measurements of CH_3OH, H_2CO and HCN agree with those from radio observations. The comet may have lost most of its volatiles during its numerous orbits around the Sun, or it may have formed closer to the young Sun than did organics-normal and organics-enriched comets.

4. Mixing ratios in Encke are consistent on different dates, but the temporal sampling of our data is insufficient for a firm conclusion as to whether its nucleus is homogeneous in the bulk. More observations of Encke are necessary to confirm its homogeneity.

In our growing database of Oort cloud and ecliptic comets, we see no correlation of chemical composition with originating dynamical reservoir or orbital period. For example, the dynamically new comet C/1999 S4 is more severely depleted than Encke, and so is the 5.4 year period (split) ecliptic comet 73P/SW 3-B and -C; while the 6.5 year period ecliptic comet 103P/Hartley 2 is normal in its composition (except for its depletion in acetylene). More comets need to be observed at infrared wavelengths, which sample primary volatiles native to the cometary nucleus, and uniquely sample the symmetric hydrocarbons. The 'organics-depleted', 'organics-normal' and 'organics-enriched' (along with 'atypical') compositional classes should be regarded as a (plausible) working hypothesis. A statistically significant sample of comets will permit us to test this classification. At present we do not know if comets currently categorized as

"depleted" or "enriched" are in fact compositional end members. Future observations would elucidate whether the current classes are well separated or if there is a more continuous distribution of abundances amongst the comet population. Measurements of cosmogonic parameters, such as spin temperature of water (indicating its formation temperature) and D/H ratios in comets, are needed in order to evaluate cometary composition as one of the keys in understanding the formation and evolution of our Solar System.

Special Acknowledgment:

This NIRSPEC investigation of comet 2P/Encke was initiated as part of our group's long-term study of cometary volatile composition, and in support of the planned 12 November 2003 encounter of Encke by the CONTOUR spacecraft (J. Veverka, Principal Investigator). The spacecraft was launched successfully on 3 July 2002, but it failed to achieve the trajectory needed to intercept the comet owing to its breakup during the orbit insertion maneuver (http://solarsystem.nasa.gov/missions/profile.cfm?MCode=CONTOUR&Display=ReadMore). But by inspiring this and other related investigations that returned new fundamental knowledge regarding this iconic comet, CONTOUR also succeeded! Thanks, Joe!

M. J. Mumma,for the Team.

General Acknowledgments:

This work was begun as part of YLR's Ph.D. dissertation at the University of Maryland, College Park, under the supervision of MJM and MFA. NASA supported YLR's Ph.D. research under the Planetary Astronomy Program (RTOP 344-32-07 to MJM), and the Astrobiology Institute

(RTOP 344-53-51 to MJM). GLV and MAD acknowledge support from NASA's Planetary Astronomy (08-PAST08-0034 to GLV, 09-PAST09-0034 to MAD) and Planetary Atmospheres (08-PATM08-0031 to GLV, 09-PATM09-0080 to MAD) Programs. BPB acknowledges support by NSF's Astronomy and Astrophysics Research Grants program NSF (1211362; 0807939) and by Cooperative Agreement NASA#NNX08AW44A. We thank Hideyo Kawakita and Reiko Furusho for their helpful feedback in preparing the observations. The data presented herein were obtained at the W. M. Keck Observatory, operated as a scientific partnership among CalTech, UCLA, and NASA. This Observatory was made possible by the generous financial support of the W. M. Keck Foundation.

References

A'Hearn, M. F., Millis, R. C., Schleicher, D. O., Osip, D. J., and Birch, P. V., 1995. The ensemble properties of comets: Results from narrowband photometry of 85 comets, 1976-1992. Icarus, 118, 223-270

A'Hearn, M. F. and 33 co-authors, 2011. EPOXI at comet Hartley 2. Science, 332, 1396-1400

Biver, N., Bockelée-Morvan, D., Crovisier, J., Lecacheux, A., Frisk, U., Hjalmarson, A., Olberg, M., Florén, H-G., Sandqvist, A., and Kwok, S., 2007. Submillimetre observations of comets with Odin: 2001–2005. Planetary and Space Science, 55, 9, 1058-1068

Bockelée-Morvan, D., Crovisier, J., Mumma, M. J., and Weaver, H. A., 2004. The composition of cometary volatiles. Comets II. Edited by Festou, M. C., Keller, H. U., and Weaver, H. A., The University of Arizona Press, Tucson, Arizona

Bonev, B., Gibb, E., Villanueva, G., Wright, K., Mumma, M., DiSanti, M., Blake, G., Magee-Sauer, K., and Salyk, C., 2009. Spin and rotational temperatures of water and methane: Comets C/2007 N3 (Lulin) and C/2007 W1 (Boattini). American Astronomical Society, DPS meeting 41, 23.07

Bonev, B. P., Mumma, M. J., Radeva, Y. L., DiSanti, M. A., Gibb, E. L., and Villanueva, G. L., 2008. The peculiar volatile composition of comet 8P/Tuttle: A contact binary of chemically distinct cometesimals. ApJ, 680, L61-L64

Bonev, B. P., 2005. Towards a chemical taxonomy of comets: infrared spectroscopic methods for quantitative measurements of cometary water, University of Toledo, dissertation

Brownlee, D., et al., 2006. Comet 81P/Wild 2 under a microscope. Science, 314 (5806), 1711-1716

Campins, H., Rieke, G. H., and Lebofsky, M. J., 1982. Infrared photometry of periodic comets Encke, Chernykh, Kearns-Kwee, Stephan-Oterma, and Tuttle. Icarus, 51, 461-465

Clough, S. A., Shephard, M. W., Mlawer, E. J., Delamere, J. S., Iacono, M. J., Cady-Pereira, K., Boukabara, S. and Brown, P. D., 2005. Atmospheric radiative transfer modeling: a summary of the AER codes, Short Communication. J. Quant. Spectrosc. Radiat. Transfer, 91, 233-244

Cochran, A. L., Barker, E. S., and Gray, C. L., 2012. Thirty years of cometary spectroscopy from McDonald Observatory. Icarus, 218, 144-168

Combi, M. R., Harris, W. M., and Smyth, W. H., 2004. Gas dynamics and kinetics in the cometary coma: Theory and observations. Comets II. Edited by Festou, M. C., Keller, H. U., and Weaver, H. A., The University of Arizona Press, Tucson, Arizona

Crovisier, J., Cometary diversity and cometary families. In XVIIIemes Rencontres de Blois: Planetary Science: Challenges and Discoveries (in press), edited by L. Celnikier (arXiv:astro-ph/0703785, 2007)

Dello Russo, N., Vervack, R. J., Jr., Lisse, C. M., Weaver, H. A., Kawakita, H., Kobayashi, H., Cochran, A. L., Harris, W. M., McKay, A. J., Biver, N., Bockelée-Morvan, D., and Crovisier, J., 2011. The volatile composition and activity of comet 103P/Hartley 2 during the EPOXI closest approach. ApJL, 734, 1, L8

Dello Russo, N., Vervack, R. J., Weaver, H. A., Kawakita, H., Kobayashi, H., Biver, N., Bockelée-Morvan, D., and Crovisier, J., 2009. The parent volatile composition of 6P/d'Arrest and a chemical comparison of Jupiter-family comets measured at infrared wavelengths. ApJ, 703, 187-197

Dello Russo, N., Vervack, R. J., Weaver, H. A., Montgomery, M. M., Deshpande, R., Fernández, Y.R., and Martin, E. L., 2008. The volatile composition of comet 17P/Holmes after its extraordinary outburst. ApJ, 680, 793-802

Dello Russo, N., Vervack, R. J., Weaver, H.A., Biver, N., Bockelée-Morvan, D., Crovisier, J., and Lisse, C. M., 2007. Compositional homogeneity in the fragmented comet 73P/Schwassmann-Wachmann 3. Nature 448, 172 – 175

Dello Russo, N., DiSanti, M. A., Magee-Sauer, K., Gibb, E. L., Mumma, M. J., Barber, R. J., and Tennyson, J., 2004. Water production and release in comet 153P/Ikeya-Zhang (C/2002 C1): accurate rotational temperature retrievals from hot-band lines near 2.9-μm. Icarus, 168, 186-200

DiSanti, M. A., Bonev, B. P., Villanueva, G. L., and Mumma, M. J., 2012. Highly depleted ethane and mildly depleted methanol in comet 21P/Giacobini-Zinner: Application of a new empirical ν_2 band model for CH_3OH near 50 K. ApJ, in press

DiSanti, M. A., and Mumma, M. J., 2008. Reservoirs for comets: compositional differences based on infrared observations. Space Sci. Rev., 138, 127-145

DiSanti, M.A., Anderson, W. M., Villanueva, G. L., Bonev, B. P., Magee-Sauer, K., Gibb, E. L., and Mumma, M. J., 2007. Depleted carbon monoxide in fragment C of the Jupiter-family comet 73P/Schwassmann-Wachmann 3. ApJ 661, L101-104

DiSanti, M.A., Villanueva, G. L., Bonev, B. P., Magee-Sauer, K., Lyke, J. E., and Mumma, M. J., 2007. Temporal evolution of parent volatiles and dust in comet 9P/Tempel 1 resulting from the Deep Impact experiment. Icarus 191, 481-493

DiSanti, M. A., Mumma, M. J., Dello-Russo, N., Magee-Sauer, K., 2001. Carbon monoxide production and excitation in comet C/1995 O1 (Hale-Bopp): Isolation of native and distributed CO sources. Icarus, 153, 361-390

Fernández, Y. R., Lowry, S. C., Weissman, P. R., Mueller, B. E. A., Samarasinha, N. H., Belton, M. J. S., and Meech, K. J., 2005. New near-aphelion light curves of comet 2P/Encke. Icarus, 175, 194-214

Fink, U., 2009. A taxonomic survey of comet composition 1985–2004 using CCD spectroscopy. Icarus, 201, 311-334

Gehrz, R. D., and Ney, E. P., 1989. Infrared photometry and spectroscopy of comet P/Encke 1987. Icarus, 80, 280-288

Gibb, E. L., DiSanti, M. A., Magee-Sauer, K., Dello Russo, N., Bonev, B. P., Mumma, M. J., 2007. The organic composition of C/2001 A2 (LINEAR) II. Search for heterogeneity within a comet nucleus. Icarus, 188, 224-232

Gladman, B., 2005. The Kuiper Belt and the Solar System's Comet Disk. Science, 307, 71-75

Fougere, N., Combi, M. R., Tenishev, V. M., Rubin, M., Bonev, B. P., and Mumma, M. J., 2011, Understanding measured rotational temperatures in the very inner coma of comet 73P/Schwassmann-Wachmann 3. EPSC Abstracts, EPSC-DPS Joint Meeting 2011, Vol. 6, 294

Hartogh, P., Lis, D. C., Bockelée-Morvan, D., de Val-Borro, M., Biver, N., Küppers, M., Emprechtinger, M., Bergin, E. A., Crovisier, J., Rengel, M., Moreno, R., Szutowicz, S., and Blake, G. A., 2011. Ocean-like water in the Jupiter-family comet 103P/Hartley 2. Nature, 478, 7368, 218-220

Jewitt, D., 2004. Looking through the HIPPO: Nucleus and dust in comet 2P/Encke. AJ, 128, 3061-3069

Jockers, K., Szutowicz, S., Villanueva, G., Bonev, T., and Hartogh, P., 2011. HCN and CN in comet 2P/Encke: Models of the non-isotropic, rotation-modulated coma and CN parent life time. Icarus, 215, 153-185

Langland-Shula, L. E., and Smith, G. H., 2011. Comet classification with new methods for gas and dust spectroscopy. Icarus, 213, 280-322

Levison, H. F., Duncan, M. J., Brasser, R., and Kaufmann, D. E., 2010. Capture of the sun's Oort cloud from stars in its birth cluster, Science, 329, 187-190

Levison, H. F., Terrell, D., Wiegert, P. A., Dones, L., and Duncan, M. J., 2006. On the origin of the unusual orbit of comet 2P/Encke, Icarus, 182, 161-168

Levison, H.F., 1996. Comet taxonomy, ASP Conference Series, 107, 173-191

Lisse, C.M., Fernández, Y.R., A'Hearn, M.F., Grün, E., Käufl, H.U., Osip, D.J., Lien, D.J., Kostiuk, T., Peschke, S.B., Walker, R.G., 2004. A tale of two very different comets: ISO and MSX measurements of dust emission from 126P/IRAS (1996) and 2P/Encke (1997). Icarus, 171, 444–462

Lowry, S., and Weissman, P., 2007. Rotation and color properties of the nucleus of comet 2P/Encke. Icarus, 188, 212-223

Magee-Sauer, K., Mumma, M. J., DiSanti, M. A., Dello Russo, N., Gibb, E. L., Bonev, B. P., and Villanueva, G. L., 2008. The organic composition of comet C/2001 A2 (LINEAR) I. Evidence for an unusual organic chemistry. Icarus, 194, 347-356

Mumma, M. J., and Charnley, S. B., 2011. The chemical composition of comets – Emerging taxonomies and natal heritage. Ann. Rev. of Astron. & Astroph., 49:471-524

Mumma, M. J., Bonev, B. P., Villanueva, G. L., Paganini, L., DiSanti, M. A., Gibb, E., Keane, J. V., Meech, K. J., Blake, G. A., Ellis, R. S., Lippi, M., Boehnhardt, H., and Magee-Sauer, K., 2011. Temporal and spatial aspects of gas release during the 2010 apparition of comet 103P/Hartley 2. ApJL, 734, L7

Mumma, M. J., Dello Russo, N., DiSanti, M. A., Magee-Sauer, K., Novak, R. E., Rettig, T., Brittain, S., Reuter, D. C., and McLean, I. S. 2001. Organic composition of C/1999 S4 (LINEAR): a comet formed near Jupiter? Science 292:1334-1339.

Mumma, M. J., DiSanti, M. A., Magee-Sauer, K., Bonev, B. P., Villanueva, G. L., Kawakita, H., Dello Russo, N., Gibb, E. L., Blake, G. A., Lyke, J. E., Campbell, R. D., Aycock, J., Conrad, A., and Hill, G. M., 2005. Parent volatiles in comet 9P/Tempel 1: Before and after impact. Science, 14, 270-274

Mumma, M. J., DiSanti, M. A., Dello Russo, N., Magee-Sauer, K., Gibb, E., and Novak, R., 2003. Remote infrared observations of parent volatiles in comets: a window on the early solar system. Adv. Space Res., 31(12), 2563-2575

Mumma, M. J., DiSanti, M. A., Dello Russo, N., Magee-Sauer, K., Rettig, T. W., 2000. Detection of CO and ethane in comet 21P/Giacobini-Zinner: Evidence for variable chemistry in the outer solar nebula. ApJ, 531, L155-L159

Ney, E., 1974. Multiband photometry of comets Kohoutek, Bennett, Bradfield, and Encke. Icarus, 23, 551-560

Paganini, L., Mumma, M. J., Bonev, B. P., Villanueva, G. L., DiSanti, M. A., Keane, J. V., and Meech, K. J., 2012. The formation heritage of Jupiter family comet 10P/Tempel 2 as revealed by infrared spectroscopy. Icarus, 218, 644-653

Radeva, Y. L., 2010. Infrared spectroscopy of parent volatiles in comets: Chemical diversity and a new fluorescence model for the ethane ν_5 band, University of Maryland, dissertation

Salyk, C., Blake, G. A., Mumma, M. J., Bonev, B. P., DiSanti, M. A., Villanueva, G. L., Radeva, Y. L., Magee-Sauer, K., and Gibb, E. L., 2007. Comet 17P/Holmes. IAU Circ., 8890, 1 (2007). Edited by Green, D. W. E.

Sekanina, Z., 1991. Encke, the comet. Royal Astronomical Society of Canada, Journal (ISSN 0035-872X), 85, 324-376

Tsiganis, K., Gomes, R., Morbidelli, A., and Levison, H. F., 2005. Origin of the orbital architecture of the giant planets of the Solar System. Nature, 435, 459-461

Villanueva, G. L., Mumma, M. J., Bonev, B. P., Novak, R. E., Barber, R. J., and DiSanti, M. A., 2012. Water in planetary and cometary atmospheres: H_2O/HDO transmittance and fluorescence models. JQSRT, 113, 202-220

Villanueva, G. L., DiSanti, M. A., Mumma, M. J., and Xu, L.-H., 2012. A quantum band model of the ν_3 fundamental of methanol (CH_3OH) and its application to fluorescence spectra of comets. ApJ 747, 37

Villanueva, G. L., Mumma, M. J., DiSanti, M. A., Bonev, B. P., Gibb, E. L., Magee-Sauer, K., Blake, G. A., and Salyk, C., 2011. The molecular composition of comet C/2007 W1 (Boattini): Evidence for a peculiar outgassing and a rich chemistry. Icarus 216, 227-240

Villanueva, G. L., Mumma, M. J., and Magee-Sauer, K., 2011. Ethane in planetary and cometary atmospheres: Transmittance and fluorescence models of the ν_7 band at 3.3 μm. JGRE 116, E08012

Villanueva, G. L., Mumma, M. J., Bonev, B. P., DiSanti, M. A., Gibb, E. L., Boehnhardt, H., and Lippi, M., 2009. A sensitive search for deuterated water in comet 8P/Tuttle. ApJ 690, L5-L9

Villanueva, G. L., Bonev, B. P., Mumma, M.J., Magee-Sauer, K., DiSanti, M. A., Salyk, C., and Blake, G. A., 2006. The volatile composition of the split ecliptic comet 73P/Schwassmann-Wachmann 3: a comparison of fragments C and B. ApJ 650, 87-90

Walsh, K. J., Morbidelli, A., Raymond, S. N., O'Brien, D. P., and Mandell, A. M. 2011, A low mass for Mars from Jupiter's early gas-driven migration, Nature, 475, 206-209

Weaver, H. A., Chin, G., Bockelée-Morvan, D., Crovisier, J., Brooke, T. Y., Cruikshank, D. P., Geballe, T. R., Kim, S. J., and Meier, R., 1999. An infrared investigation of volatiles in comet 21P/Giacobini-Zinner. Icarus, 142, 2, 482-497

Weaver, H. A., Mumma, M. J., 1984. Infrared molecular emissions from comets. ApJ, 276, 782-797

Weiler, M., 2012. The chemistry of C_3 and C_2 in cometary comae. I. Current models revisited. Astron. & Astrophys. 538, A149, 1-12

Xie, X., and Mumma, M.J., 1992. The effect of electron collisions on rotational populations of cometary water. ApJ 386, 720-728

Xie, X., and Mumma, M.J., 1996. Monte Carlo simulation of cometary atmospheres: application to comet P/Halley at the time of the Giotto Spacecraft encounter. I. Isotropic Model. ApJ 464, 442-456

Xie, X., and Mumma, M.J., 1996. Monte Carlo simulation of cometary atmospheres: application to comet P/Halley at the time of the Giotto Spacecraft encounter. II. Axisymmetric Model. ApJ 464, 457-475

Yamamoto, T., 1985. Formation environment of cometary nuclei in the primordial solar nebula. Astron. Astrophys. 142, 31-36

Yang, B., Jewitt, D., Schelte, B. J., 2009. Comet 17/P/Holmes in outburst: The near infrared spectrum. AJ, 137, 5, 4538-4546

Table 1: Log of Observations of comet Encke.

UT Time (2003)	Integration time [min]	Setting[I]	Frequency range of setting [cm^{-1}]	R_h[II] [AU]	Δ[II] [AU]	Δ_{dot}[II] [km s^{-1}]
4 Nov., 5:09-7:17	84	KL2	3464 – 2759	1.210	0.313	-13.59
9:29-9:52	20	KL1	3521 – 2833	1.208	0.312	-13.19
5 Nov., 7:23-8:30	48	KL1	3521 – 2833	1.194	0.305	-12.45
9:31-10:05	12	MW_A	2162 - 1996	1.193	0.304	-12.25
6 Nov., 4:40-6:21	80	KL2	3464 – 2759	1.180	0.299	-11.78
9:18-9:50	14	MW_A	2162 - 1996	1.178	0.297	-11.31

[I]The KL1 setting simultaneously samples CH_3OH, C_2H_6 & H_2O. The KL2 setting simultaneously samples HCN, CH_4, C_2H_2, C_2H_6, H_2CO & H_2O; and the MW_A setting simultaneously samples CO & H_2O.

[II]R_h is the heliocentric distance, Δ is the geocentric distance, and Δ_{dot} is the line-of-sight velocity.

Table 2. Production rates and mixing ratios of volatiles in 2P/Encke.[I]

Setting / Time on Source	Molecule (T_{rot})	Global Q [10^{25} s^{-1}]	Mixing Ratio %
4 Nov. 2003			
KL1 / 20 min	H_2O ($29\ ^{-7}/_{+10}$ K)	215.7 ± 25.3	100.00
	C_2H_6 ν_7 (29 K)	0.7 ± 0.1	0.32 ± 0.05
	CH_3OH (29 K)	8.5 ± 1.5	3.93 ± 0.69
KL2 / 84 min	H_2O (29 K)	272.2 ± 86.7	100.00
	H_2CO (29 K)	< 0.4 at 3σ	< 0.13 at 3σ
	C_2H_6 ν_5 (29 K)	1.0 ± 0.4	0.36 ± 0.09
	CH_4 (29 K)	0.9 ± 0.4	0.31 ± 0.11
	HCN (29 K)	0.4 ± 0.1	0.13 ± 0.03
	C_2H_2 (29 K)	< 0.3 at 3σ	< 0.10 at 3σ
5 Nov. 2003			
KL1 / 48 min	H_2O ($30\ ^{-2}/_{+2}$ K)	298.0 ± 23.9	100.00
	C_2H_6 ν_7 (29 K)	0.9 ± 0.1	0.31 ± 0.04
	CH_3OH ($24\ ^{-5}/_{+6}$ K)	9.1 ± 1.0	3.01 ± 0.28
	CH_3OH (30 K)	10.2 ± 1.0	3.40 ± 0.29

MWA Combined 12 min (Nov. 5) & 14 min (Nov. 6)[I]	H_2O (30 K)[II]	321.8 ± 82.0	100.00
	CO (30 K)[II]	< 5.7 at 3σ	< 1.77 at 3σ
6 Nov. 2003			
KL2 / 80 min	H_2O (30 K)	256.4 ± 20.4	100.00
	H_2CO (30 K)	< 0.3 at 3σ	< 0.13 at 3σ
	C_2H_6 ν_5 (30 K)	< 0.6 at 3σ	< 0.23 at 3σ
	CH_4 (30 K)	1.3 ± 0.7	0.52 ± 0.28
	HCN ($20^{-8}/_{+16}$ K)	0.18 ± 0.03	0.07 ± 0.01
	HCN (30 K)	0.21 ± 0.04	0.08 ± 0.01
	C_2H_2 (30 K)	< 0.2 at 3σ	< 0.08 at 3σ

[I]Production rates for H_2O assume an equilibrium Ortho-to-Para ratio of 3.0. Detailed analysis of the OPR in comet Encke is reserved for a further publication.

[II]The production rates of H_2O and CO for MW_A are based on data from 5 Nov. (12 min on source) and 6 Nov. (14 min on source), which were combined to provide a higher signal to noise ratio.

Table 3. Mixing ratios in 2P/Encke, in other Jupiter-family comets; and in 'organics-depleted' and 'organics-enriched' end-member Oort Cloud comets.

Mixing Ratios in a Sample of Jupiter-family Comets							
Comet	**CH_3OH**	**HCN**	**H_2CO**	**C_2H_2**	**C_2H_6**	**CH_4**	**CO**
73P/S-W 3-C[I]	0.149 ± 0.029	0.242 ± 0.014	0.147 ± 0.033	0.049 ± 0.020	0.107 ± 0.011	< 0.25	0.5 ± 0.13
21P/Giacobini-Zinner[II]	1.22 ± 0.11	< 0.27	< 0.8	< 0.42	0.136 ± 0.023	-	10.25 ± 5.80
9P/Tempel 1[III] (pre-impact)	1.3 ± 0.2	0.18 ± 0.06	-	-	0.23 ± 0.04	-	-
9P/Tempel 1[III] (post-impact, including ejecta)	0.99 ± 0.17	0.22 ± 0.03	-	0.13 ± 0.04	0.40 ± 0.04	0.54 ± 0.30	4.3 ± 1.7
6P/d'Arrest[IV]	1.42 ± 0.30	0.034 ± 0.008	0.36 ± 0.09	< 0.052	0.256 ± 0.061	-	-
10P/Tempel 2[V]	1.58 ± 0.23	0.13 ± 0.02	< 0.11	< 0.07	0.39 ± 0.04	-	-
103P/Hartley 2[VI]	2.28 ± 0.38	0.26 ± 0.02	0.23 ± 0.05	0.08 ± 0.01	0.75 ± 0.07	< 1.2	-
17P/Holmes[VII]	3.0 ± 1.0	0.538 ± 0.075	-	0.344 ± 0.053	1.90 ± 0.54	-	-
2P/Encke[VIII]	3.48 ± 0.27	0.09 ± 0.01	< 0.13	< 0.08	0.32 ± 0.03	0.34 ± 0.10	< 1.77
Mixing Ratios in End-Member Oort Cloud Comets							
C/1999 S4[IX] (Organics-Depleted)	< 0.15	0.10 ± 0.03	-	< 0.12	0.11 ± 0.02	0.18 ± 0.06	0.9 ± 0.3
C/2001 A2[X] (Organics-Enriched)	3.9 ± 0.4	0.6 ± 0.1	0.24 ± 0.05	0.5 ± 0.1	1.7 ± 0.2	1.2 ± 0.2	3.9 ± 1.1

C/2007 W1 (Boattini)[XI]	3.69	0.50	< 0.12	0.29	1.97	1.57	4.50
(Organics-Enriched)	± 0.07	± 0.01		± 0.02	± 0.03	± 0.16	± 0.51

[I]Dello Russo et al. 2007 (C_2H_6, C_2H_2, HCN, H_2CO & CH_3OH, 14.5 May 2006), Villanueva et al. 2006 (CH_4, 7 Apr. 2006), DiSanti et al. 2007a (CO, 27 & 30 May 2006).

[II]Weaver et al. 1999 (C_2H_2, HCN, H_2CO, Oct. 25-29 1998), Mumma et al. 2000 (CO, Oct. 2-10 1998) & DiSanti et al. 2012 (C_2H_6 & CH_3OH, Jun. 3 2005).

[III]Mumma et al. 2005 (Jun. 3 2005 & Jul. 4-5 2005), DiSanti et al. 2007b (4 Jul. 2005), DiSanti and Mumma 2008.

[IV]Dello Russo et al. 2009 (11 Aug. 2008).

[V]Paganini et al. 2012 (26 Jul. 2010).

[VI]Mumma et al. 2011 (22 Oct. 2010, mixing ratios in agreement with those presented for other dates; CH_4 is for 16 Nov.).

[VII]Dello Russo et al. 2008 (27 & 31 Oct. 2007).

[VIII]This work. Values are weighted means from different dates; 3-σ upper limits are provided where indicated.

[IX]Mumma et al. 2003 (13 Jul. 2000).

[X]Magee-Sauer et al. 2008 & Gibb et al. 2007 (9 & 10 Jul., 4 & 10 Aug. 2001).

[XI]Villanueva et al. 2011a (9 & 10 Jul. (weighted means), mixing ratios relative to symmetric water).

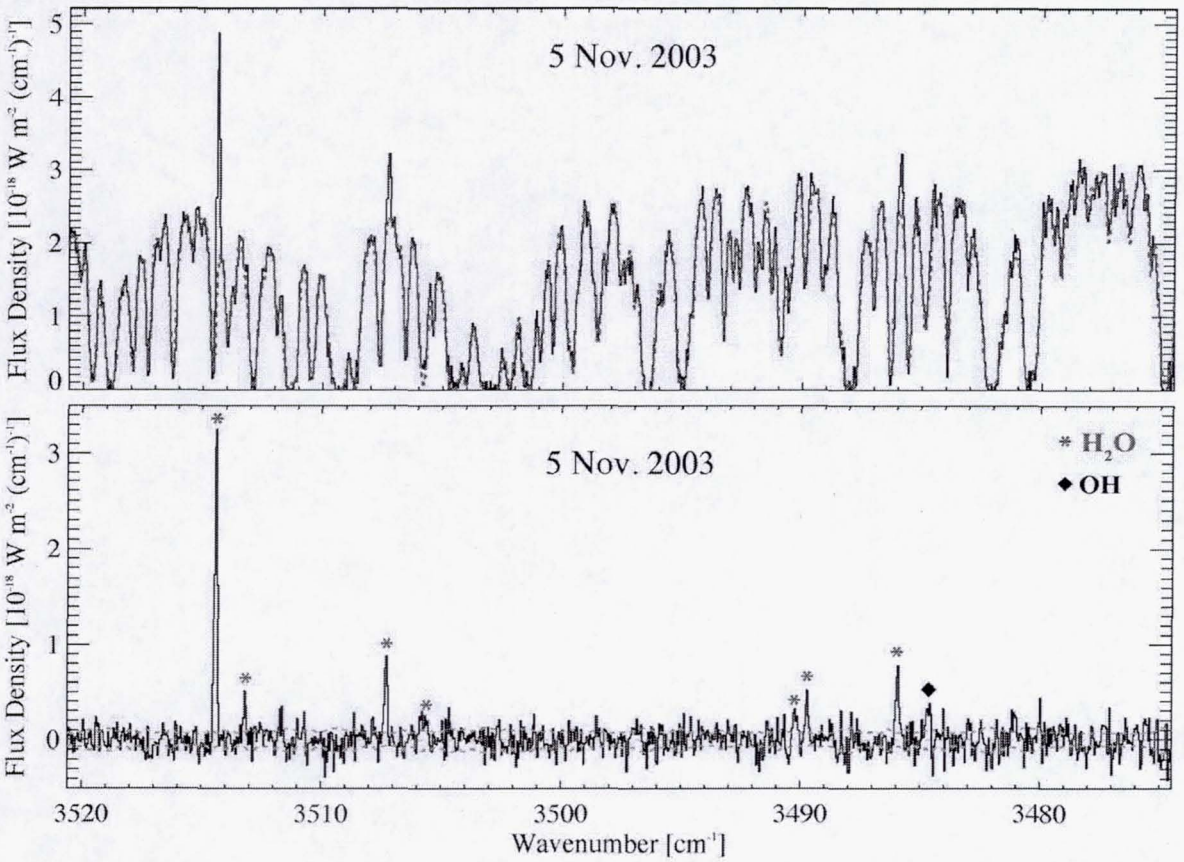

Figure 1: 2P/Encke cometary spectrum and superimposed terrestrial transmittance model (dashed line) for KL1, Order 27, on 5 Nov. 2003 (upper panel), and residual spectrum (lower panel). Spectral lines of H_2O, OH, and blends are seen. The flux density scale is shown at left, and the (± 1-σ) noise envelope is shown as dashed lines centered on zero flux density, in each panel.

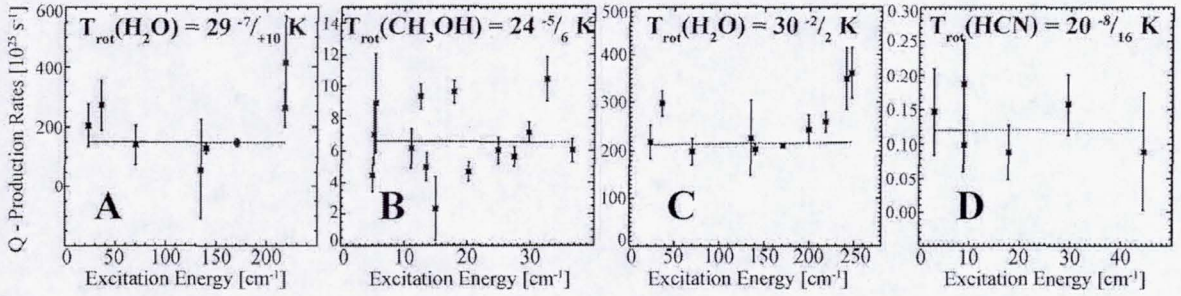

Figure 2: Excitation analysis for H_2O on 4 Nov. (Panel A), CH_3OH on 5 Nov. (Panel B), H_2O on 5 Nov. (Panel C), and HCN on 6 Nov. (Panel D). At the retrieved T_{rot}, the agreement among production rates derived from individual measured lines is satisfactory, for each species. Rotational temperatures for H_2O in the KL1 setting (Panels A & C) are retrieved from the combination of spectral lines in echelle orders 26 and 27.

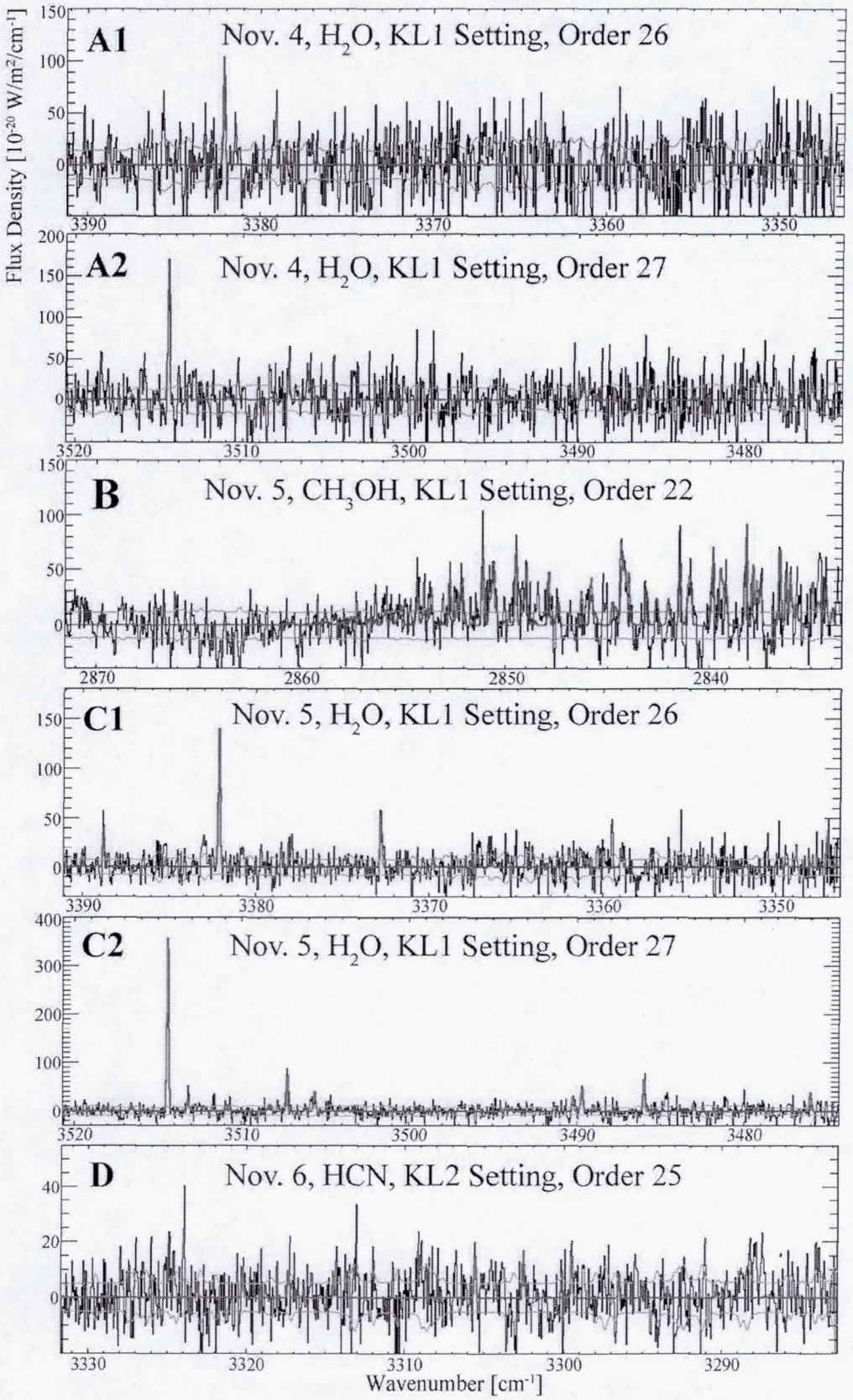
A1
Nov. 4, H2O, KL1 Setting, Order 26
A2
Nov. 4, H2O, KL1 Setting, Order 27
B
Nov. 5, CH3OH, KL1 Setting, Order 22
C1
Nov. 5, H2O, KL1 Setting, Order 26
C2
Nov. 5, H2O, KL1 Setting, Order 27
D
Nov. 6, HCN, KL2 Setting, Order 25
Flux Density [10-20 W/m2/cm-1]
Wavenumber [cm-1]

Figure 3: Residual features for H_2O on 4 Nov. (Panel A1 for Order 26 & Panel A2 for Order 27); CH_3OH on 5 Nov. (Panel B), H_2O on 5 Nov. (Panel C1 for Order 26 & Panel C2 for Order 27), and HCN on 6 Nov. (Panel D), with the fluorescence model for each molecule superimposed in red. The combination of spectral lines sampled in orders 26 and 27 for H_2O on 5 Nov. resulted in the best-constrained T_{rot} of $30\ ^{-2}/_{+2}$ K.

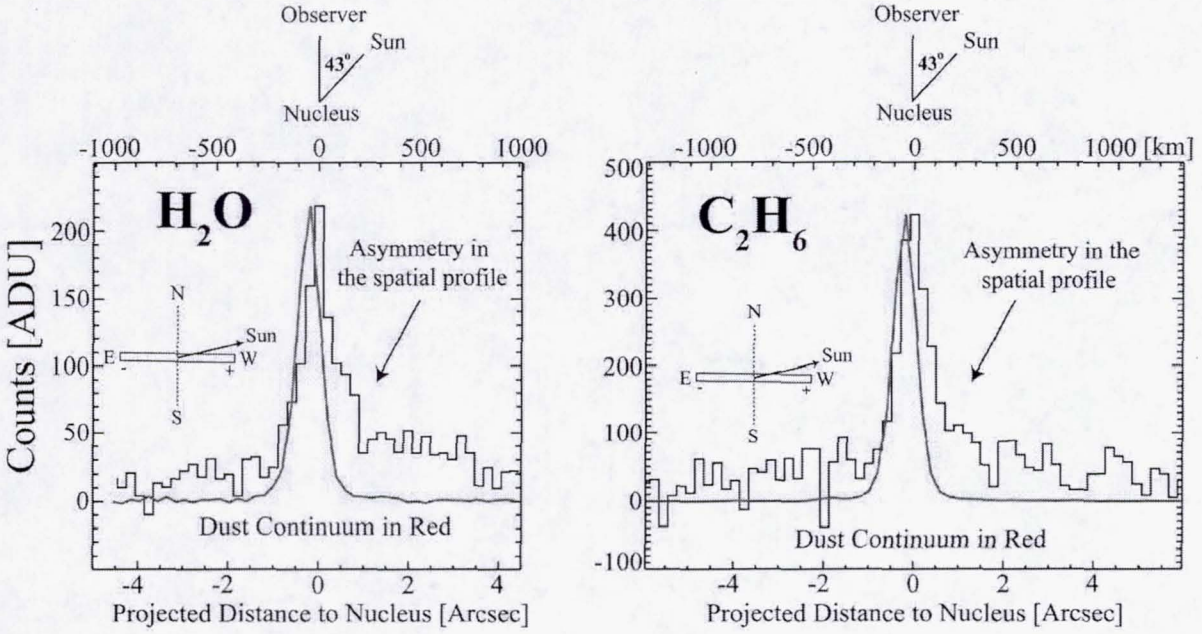

Figure 4: Emission spatial profiles for H_2O and C_2H_6 (KL1 setting, Nov. 5) in black, and dust continuum in red. Asymmetry in the spatial profile is compensated by extracting production rates on both sides of the profile, and reporting an averaged global production rate. The continuum profile is clearly displaced from the gas profile, suggesting preferential outgassing towards the sun. The orientation of the instrument slit (89°) is shown on the sky plane, as well as the aspect in the Sun-Nucleus-Observer plane.

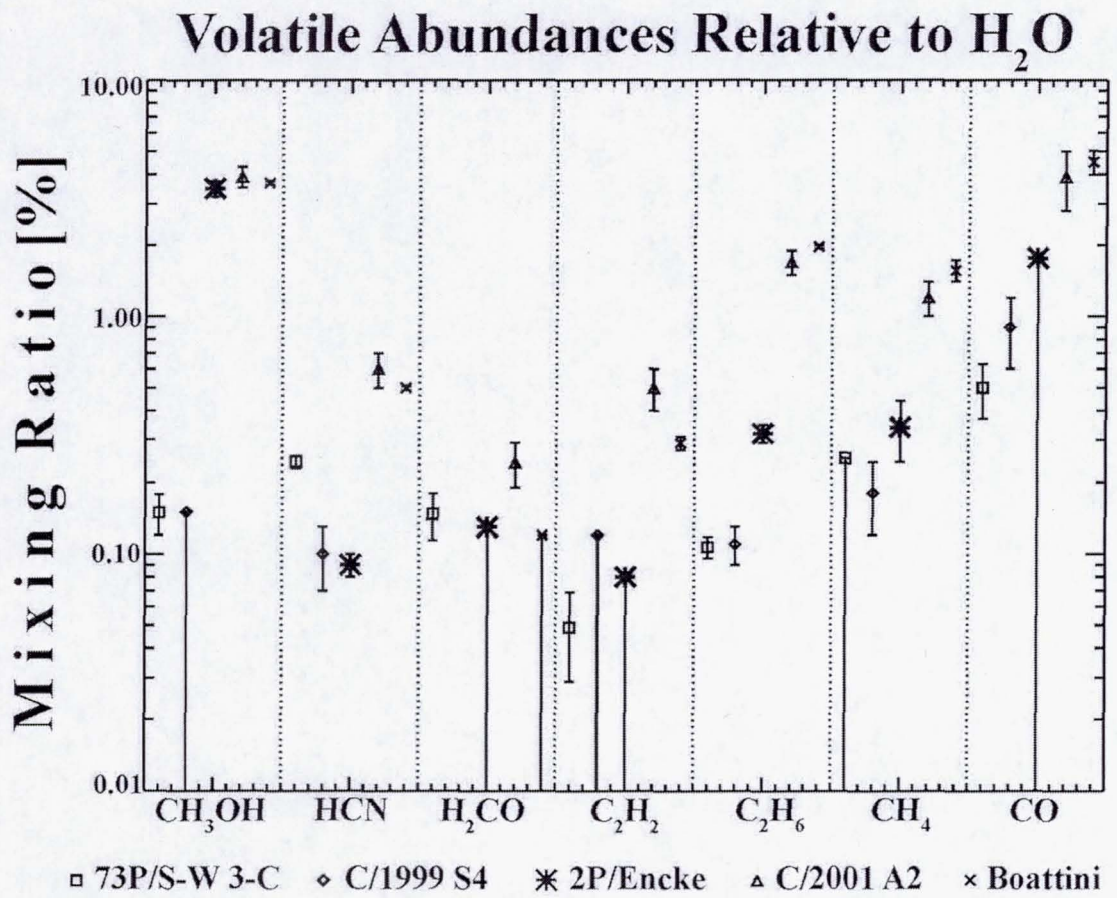

Figure 5: Comparison among mixing ratios of organic species in the severely depleted ecliptic comet 73P/S-W 3-C, the severely depleted Oort cloud comet C/1999 S4, the ecliptic comet Encke, and the enriched Oort cloud comets C/2001 A2 and C/2007 W1 (Boattini). Organic species are presented on the figure in terms of decreasing sublimation temperature (from left to right). Comet Encke is enriched in CH_3OH; and depleted in HCN, H_2CO, C_2H_2, C_2H_6, CH_4 & CO.

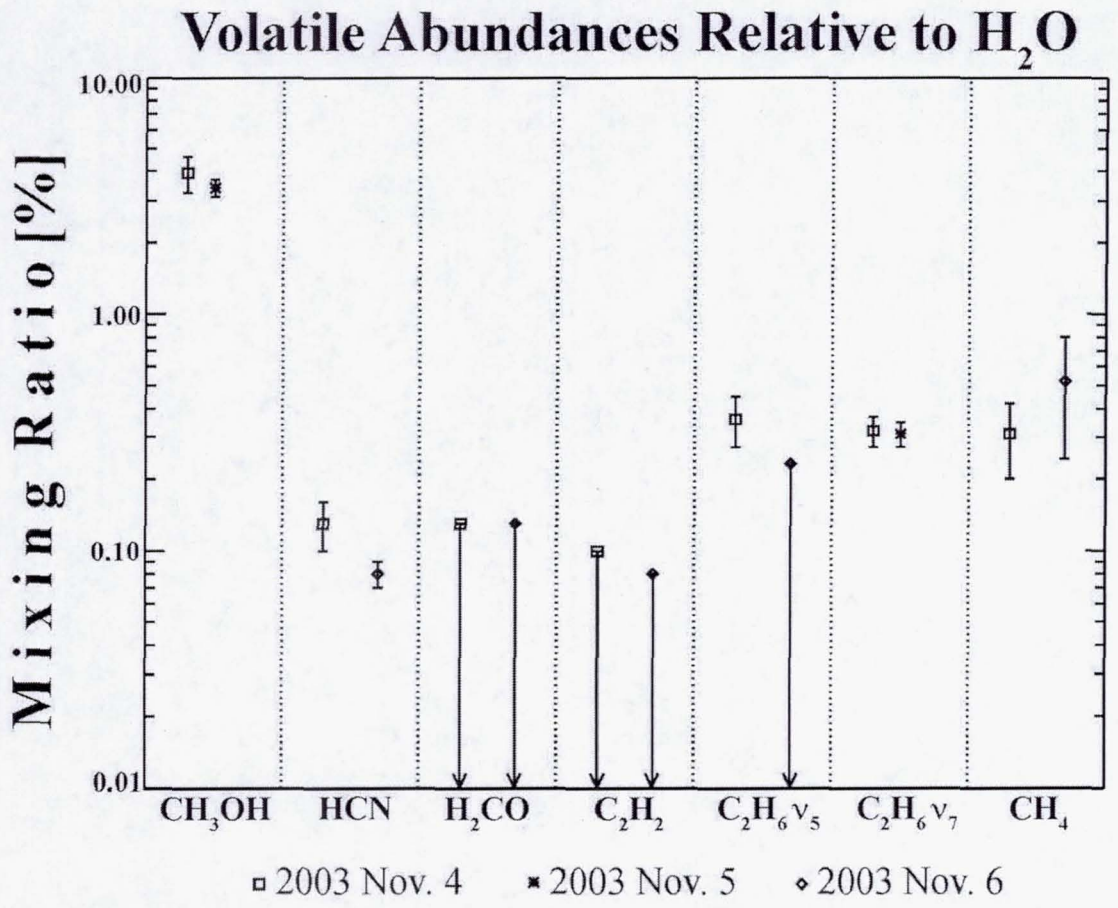

Figure 6: Agreement among mixing ratios of organic species in 2P/Encke on 4-6 Nov. 2003, within 1-σ (2-σ for HCN). The lack of variability would suggest homogeneity of Encke's nucleus, however, we lack sufficient temporal sampling to make a firm conclusion.